




CASE REPORT

Epithelial–mesenchymal transition in an EcPV2-positive vulvar squamous cell carcinoma of a mare

Livia De Paolis¹  | Federico Armando² | Vittoria Montemurro³ | Lucio Petrizzi⁴ | Paola Straticò⁴ | Samanta Mecocci⁵ | Chiara Guarnieri⁶  | Marzia Pezzolato³ | Floriana Fruscione¹ | Benedetta Passeri⁶ | Giuseppe Marruchella⁴  | Elisabetta Razzuoli¹

¹Istituto Zooprofilattico Sperimentale del Piemonte, Liguria e Valle D'Aosta, National Reference Center of Veterinary and Comparative Oncology (CEROVEC), Genova, Italy

²Department of Pathology, University of Veterinary Medicine Hannover, Hannover, Germany

³Istituto Zooprofilattico Sperimentale del Piemonte, Liguria e Valle D'Aosta, Histopathology and Applied Technology Laboratory, Torino, Italy

⁴Faculty of Veterinary Medicine, University of Teramo, Teramo, Italy

⁵Department of Veterinary Science, University of Perugia, Perugia, Italy

⁶Department of Veterinary Science, University of Parma, Parma, Italy

Correspondence

Federico Armando, Department of Pathology, University of Veterinary Medicine Hannover, Hannover, Germany.
Email: federico.armando@tiho-hannover.de

Funding information

Italian Ministry of Health, Grant/Award Number: IZS PLV 15/18 RC; Region of Liguria, Grant/Award Number: 22L03; Deutsche Forschungsgemeinschaft, Grant/Award Number: 491094227; University of Veterinary Medicine Hannover Foundation

Abstract

Background: Vulvar squamous cell carcinoma (VSCC) has been recently associated with *Equus caballus* papillomavirus type 2 (EcPV2) infection. Still, few reports concerning this disease are present in the literature.

Objective: To describe a case of naturally occurring EcPV2-induced VSCC, by investigating tumour ability in undergoing the epithelial-to-mesenchymal transition (EMT).

Study design: Case report.

Methods: A 13-year-old Haflinger mare was referred for a rapidly growing vulvar mass. After surgical excision, the mass was submitted to histopathology and molecular analysis. Histopathological diagnosis was consistent with a VSCC. Real-time qPCR, real-time reverse transcriptase (RT)-qPCR and RNAscope were carried out to detect EcPV2 infection and to evaluate E6/E7 oncogenes expression. To highlight the EMT, immunohistochemistry (IHC) was performed. Expression of EMT-related and innate immunity-related genes was investigated through RT-qPCR.

Results: Real-time qPCR, RT-qPCR and RNAscope confirmed EcPV2 DNA presence and expression of EcPV2 oncoproteins (E6 and E7) within the neoplastic vulvar lesion. IHC highlighted a cadherin switch together with the expression of the EMT-related transcription factor HIF1 α . With RT-qPCR, significantly increased gene expression of EBI3 (45.0 ± 1.62 , $p < 0.01$), CDH2 (2445.3 ± 0.39 , $p < 0.001$), CXCL8 (288.7 ± 0.40 , $p < 0.001$) and decreased gene expression of CDH1 (0.3 ± 0.57 , $p < 0.05$), IL12A (0.04 ± 1.06 , $p < 0.01$) and IL17 (0.2 ± 0.64 , $p < 0.05$) were detected.

Main limitations: Lack of ability to generalise and danger of over-interpretation.

Conclusion: The results obtained were suggestive of an EMT event occurring within the neoplastic lesion.

KEYWORDS

epithelial–mesenchymal transition (EMT), *Equus caballus* papillomavirus type 2 (EcPV2), horse, vulvar squamous cell carcinoma (VSCC)

This is an open access article under the terms of the [Creative Commons Attribution](https://creativecommons.org/licenses/by/4.0/) License, which permits use, distribution and reproduction in any medium, provided the original work is properly cited.

© 2023 The Authors. *Equine Veterinary Journal* published by John Wiley & Sons Ltd on behalf of EVJ Ltd.

1 | INTRODUCTION

Squamous cell carcinoma (SCC) represents one of the most common malignant cutaneous tumours in horses, accounting for 7%–37% of all skin tumours. Although SCC can arise from any skin and mucosal site, it most commonly affects non-pigmented skin and muco-cutaneous junctions, such as eyelids and external genitalia.¹ Human papillomavirus (HPV) infections are regarded as the primary causative agents of cervical, anogenital and head and neck SCCs.² Likewise equine papillomaviruses (EcPVs) could play a pivotal role in the aetiology and pathogenesis of SCCs³ (penile, vulvar, clitoral, gastric, oropharyngeal papillomas and SCCs).^{4–6}

Epithelial-mesenchymal transition (EMT) can be defined as a complex process leading to the trans-differentiation of epithelial cells into motile mesenchymal cells. EMT phenotype is crucial in different physiological and disease events, including embryogenesis, wound healing, stem cell behaviour, fibrosis and cancer progression.^{7,8} A growing body of evidence indicates that EMT is activated in various cancer types, thus triggering key features of neoplastic cells (i.e., their ability to invade tissues and to form metastasis).^{7,9} EMT is a multistep process and causes both morphological and molecular changes in neoplastic epithelial cells, which decrease the expression of epithelial markers (e.g., E-cadherin) while increasing the expression of mesenchymal markers (e.g., N-cadherin). Moreover, core EMT programs involving EMT transcription factors (e.g., TWIST and ZEB), miRNAs and epigenetic regulators drive carcinogenesis.¹⁰ As a result, during EMT neoplastic epithelial cells lose cell-to-cell adhesion and gradually acquire the ability to migrate through the extracellular matrix, gaining invasiveness.¹¹ In human medicine, the relevance of EMT in cancer progression has been investigated for decades.¹² Interestingly, it has been hypothesised that papillomaviral oncoproteins (namely, E6 and E7) could activate EMT in HPV-associated carcinomas.¹³

Data from investigation of the EMT process in relation to the EcPV2 infectious status in equine VSCC are still missing: some recent data suggest that penile and laryngeal EcPV2-associated SCC may undergo EMT, most likely after the activation of the canonical wnt/ β -catenin pathway.^{14–17} Considering that, the current report aims to describe the main pathological and virological features of an equine vulvar SCC with special emphasis on the EMT process.

2 | MATERIALS AND METHODS

2.1 | Clinical history and samples' collection

In September 2022, a 13-year-old Haflinger mare was referred to the Veterinary Teaching Hospital of Teramo with a history of rapidly growing vulvar mass. On clinical examination, a large, firm and ulcerated lesion was observed, which severely affected the external genitalia (Figure 1). The horse was sedated with a bolus of detomidine and butorphanol, caudal epidural anaesthesia was performed with detomidine and morphine. Thereafter, the urinary bladder was catheterised and the mass was surgically excised with the standing mare restrained in



FIGURE 1 Vulvar mass affecting a 13-year-old Haflinger mare.

stocks. The abnormal tissue was removed to the muco-cutaneous junction and representative tissue samples were collected from the vulvar lesion (VL) and from the surrounding, seemingly healthy skin (HS). Seven samples were obtained from each tissue (VL and HS). One sample from the VL and HS was fixed in 10% neutral buffered formalin, embedded in paraffin and routinely processed for histological, immunohistochemical and RNAscope investigations (haematoxylin and eosin stain, H&E). Six other tissue samples from each tissue type (VL and HS) were snap frozen and stored at -80°C for further analysis (DNA and RNA tests).

2.2 | Real-time qPCR to detect EcPV2 genes

Total DNA was extracted from three frozen tissue samples per tissue type (VL and HS) using the QIAamp DNA Mini Kit (Qiagen), according to the manufacturer's instructions, and quantified by Qubit fluorimeter (Thermo Fisher Scientific). The presence of EcPV2 -L1, -E2, -E6 and -E7 was assessed in a CFX96 Real-Time System (Bio-Rad), using primers and related specific probes (Table S1) as previously described.¹⁸

2.3 | RNAscope

RNAscope (Advanced Cell Diagnostics, ACD) was performed using probes targeting E6/E7 oncogenes of EcPV2 on VL and HS slides according to the manufacturer's protocol. Briefly, FFPE samples were hybridised with E6/E7 V-EcPV2 RNAscope[®] probe. Six amplifying solutions were used for each amplification steps: AMP-1, AMP-3 and AMP-5 for 15 min each, AMP-2, AMP-4 and AMP-6 for 30 min.

Amplified signal was detected using Fast RED (Advanced Cell Diagnostics), then nuclei were counterstained with Gill's haematoxylin.

The presence of E6/E7 signals was evaluated with a Zeiss Axio Scope A1 microscope (Zeiss) at increasing magnifications (10×, 20× and 40×).

2.4 | Reverse transcriptase (RT)-qPCR to evaluate EcPV2 and host gene expression

Total RNA was extracted from other three frozen tissue samples per tissue type (VL and HS), using the RNeasy Mini Kit (Qiagen), following the manufacturer's instructions. SuperScript™ IV VILO™ Master Mix (Invitrogen, Thermo Fisher Scientific) was used to reverse-transcribe 500 ng of total RNA from each sample. L1 and E6 viral genes expression was performed as previously described. RNA was used as control, to exclude DNA contamination.

Host gene expression was assessed in a CFX96™ Real-Time System using Power SYBR™ Green PCR Master Mix (Applied Biosystems, Thermo Fisher Scientific) according to the manufacturer's instructions. B2M was used as reference gene.¹⁵ Primers sets are reported in Table S2. They were derived from previous studies^{14,15,19} or designed including an intron or spanning an exon-exon junction through Primer3web tool v.4.1.0 (<https://primer3.ut.ee>). Differences in VL and HS samples were calculated with the $2^{(-\Delta\Delta Cq)}$ method. Data were checked for normal distribution and submitted to Kruskal-Wallis test followed by Dunn's post hoc test.

2.5 | Immunohistochemical investigations

Immunohistochemistry (IHC) was conducted on FFPE samples (both VL and HS) to estimate tumour's proliferation index and to evaluate EMT, as previously described.^{15,20} Briefly, primary antibodies for Ki67, E-cadherin, β -catenin, vimentin, N-cadherin, HIF1 α and pancytokeratin AE1/AE3 were used (Table S3). Immune reactions were detected using an avidin-biotin peroxidase kit (Vectastain, Elite, ABC-Kit PK-6100, Vector Labs) amplification method and visualised using 3,3'-Diaminobenzidine tetrahydrochloride (DAB) (DAB-Kit-SK4100, Vector Labs), while counterstaining was performed with Meyer's haematoxylin.

In VL and HS samples, EMT markers and Ki67 were manually quantified counting immune reactive cells in 10 high-power fields (final magnification 400×), randomly distributed throughout the tumour invasive front. Digital pictures were kept using a Nikon Eclipse E800 microscope (Nikon Corporation), provided with a Nikon PLAN APO lens and equipped with a Camera DIGITAL SIGHT DS-Fi1 (Nikon Corporation).

2.6 | Data analysis

Data were analysed for normal distribution with the Shapiro-Wilk test, followed by the Mann-Whitney test. Statistical significance was set at a p value ≤ 0.05 (GraphPad Software).

3 | RESULTS

3.1 | Surgical excision and clinical outcome

The horse recovered uneventfully from surgery and sedation. Six hours after surgery pain was shown and treated with non-steroidal anti-inflammatory drugs. Normal urination was observed within 8 h from the end of the surgical procedure. Seven months follow-up, the mare is in good condition and with no macroscopic growing mass at the vulvar region suggesting tumour recurrence.

3.2 | Histopathological investigations

Microscopically, the VL skin was multifocally ulcerated, hyperaemic and haemorrhagic, with a dense inflammatory reaction mostly consisting of neutrophils. Nests, islands and cords of neoplastic epithelial cells were seen in all VL samples, deeply infiltrating the submucosa and subcutis. Neoplastic lobules were usually surrounded by a layer of basaloid cells, while varying and disorderly degrees of keratinisation were observed in their central portions (Figure 2A). Occasionally, such lobules resembled cystic spaces, lined by neoplastic cells, and filled with proteinaceous fluid and necrotic cells (Figure 2B). Intercellular bridges and keratin pearls were very evident. Mitotic figures were common (0–3 per high power field, final magnification 400×) and often atypical. The neoplastic proliferation was intermingled with a prominent desmoplastic reaction, which clearly prevailed in some areas (Figure 2C). Multiple neoplastic nests were surrounded by a thick, hyaline basement membrane, interposed between the stroma and the neoplastic epithelial cells (Figure 2D). No evidence of neoplasia was observed in samples taken from HS. Therein, scattered foci of perivascular/peri-glandular inflammation were observed, with infiltration of lymphocytes and plasma cells. Considering the above-mentioned findings, the diagnosis of SCC was made.

3.3 | Detection of EcPV2 genes

qPCR tests demonstrated the presence of EcPV2-L1, -E6 and -E7 genes, both in VL and HS samples (Table 1).

3.4 | EcPV2 and host gene expression

RT-qPCR revealed the expression of EcPV2-L1 and -E6 genes in VL sample (Table 1). HS yielded negative results for oncogene expression (Table 1); data were confirmed by RNAscope (Figure S1).

Data regarding host gene expression are reported in Table 2. The following genes showed a significantly higher expression in VL when compared with HS: *EBI3* ($p < 0.01$), *CDH2* ($p < 0.001$) and *CXCL8* ($p < 0.001$). On the contrary, genes *CDH1* ($p < 0.05$), *IL12A* ($p < 0.01$) and *IL17* ($p < 0.05$) revealed a significant decreased expression in VL compared with HS.

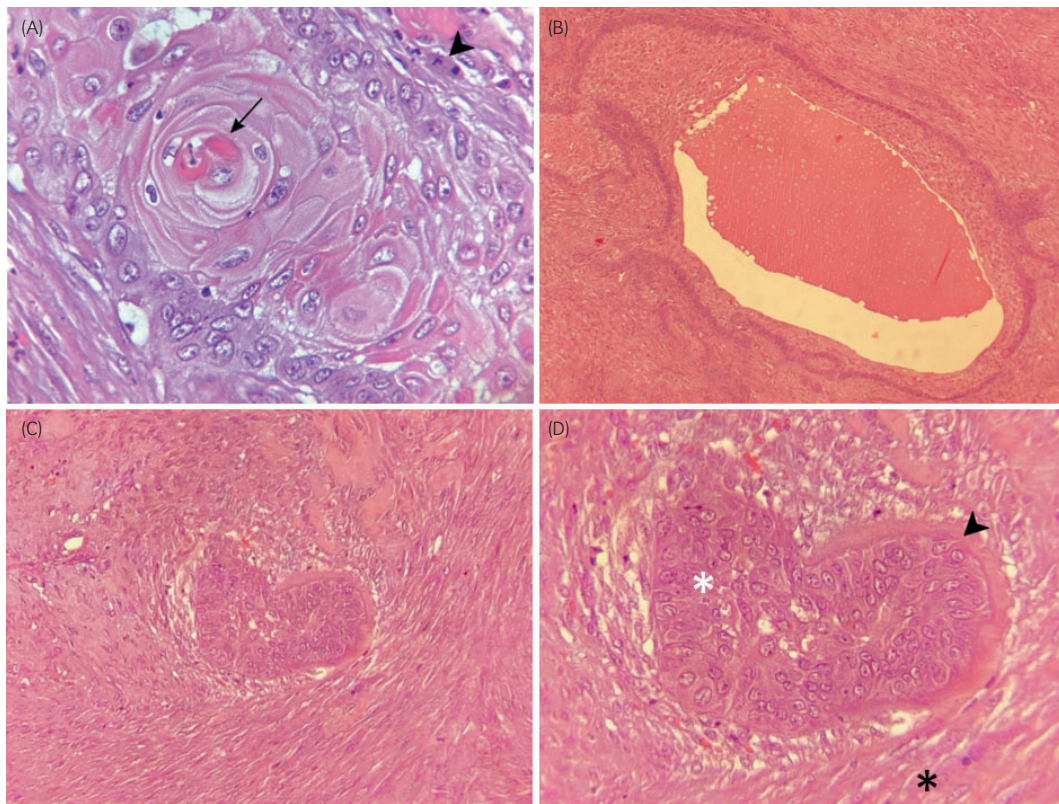


FIGURE 2 Overview of the vulvar squamous cell carcinoma histological findings: (A) A small cluster of cells undergoing keratinisation (arrow); an atypical mitotic figure is also present (arrowhead). (B) A cystic space, lined by neoplastic cells and filled with eosinophilic proteinaceous material and necrotic cells. (C) A neoplastic nest intermingled with a prominent desmoplastic reaction. (D) Higher magnification from (C), the neoplastic nest appears surrounded by a thick, hyaline basement membrane (arrowhead), separating the stroma (black asterisk) from the neoplastic epithelial cells (white asterisk).

TABLE 1 Results obtained from real-time polymerase chain reaction (PCR) and reverse transcriptase (RT)-quantitative (q)PCR.

Sample	qPCR					RT-qPCR	
	EcPV2-L1	EcPV2-E2	EcPV2-E6	EcPV2-E7	Eq-B2M	L1	E6
Healthy skin (HS)	28.0 ± 1.34	>38	29.3 ± 1.0	29.1 ± 1.0	27.7 ± 0.6	>38	>38
Vulvar lesion (VL)	25.8 ± 0.8	>38	26.7 ± 0.3	26.8 ± 0.2	26.9 ± 0.7	35.5 ± 1.2	31.1 ± 1.5

Note: Data are expressed as mean value between the three HS and neoplastic VL samplings ± standard deviation.

3.5 | Immunohistochemistry

Immunohistochemical analysis for pan-cytokeratin AE1/AE3 highlighted a significant ($p < 0.001$) lower number of cells expressing cytoplasmic cytokeratins in VL when compared with HS (Figure 3A,C). Conversely, the cytoplasmic vimentin expression was significantly higher ($p < 0.0001$) in VL compared with HS (Figure 3B,D). Immunohistochemical analysis revealed a significant ($p < 0.001$) lower number of cells expressing E-cadherin at a membranous level in VL with respect to HS (Figure 4A,C). Interestingly, the overall number of cells expressing N-cadherin was significantly ($p < 0.001$) higher in VL compared with HS, both at a membranous and cytoplasmic level (Figure 4B,D). In addition, the neoplastic VL showed a significant ($p < 0.005$) lower number of cells expressing β -catenin at a membranous level when compared

TABLE 2 p value determining the level of statistical significance in gene expression from healthy skin and neoplastic vulvar lesion.

Gene	$2^{-(\Delta\Delta Cq)} \pm$ standard error (SE) (p value)
CDH1	0.3 ± 0.57*
CDH2	2445.3 ± 0.39***
EBI3	45.0 ± 1.62**
IL12A	0.04 ± 1.06**
IL17	0.2 ± 0.64*
CXCL8	288.7 ± 0.40***

Note: Data are expressed as $2^{-(\Delta\Delta Cq)} \pm$ SE. Differences were evaluated through the Kruskal-Wallis test and applying the post hoc Dunn's multiple comparison test.

* $p < 0.05$. ** $p < 0.01$. *** $p < 0.001$.

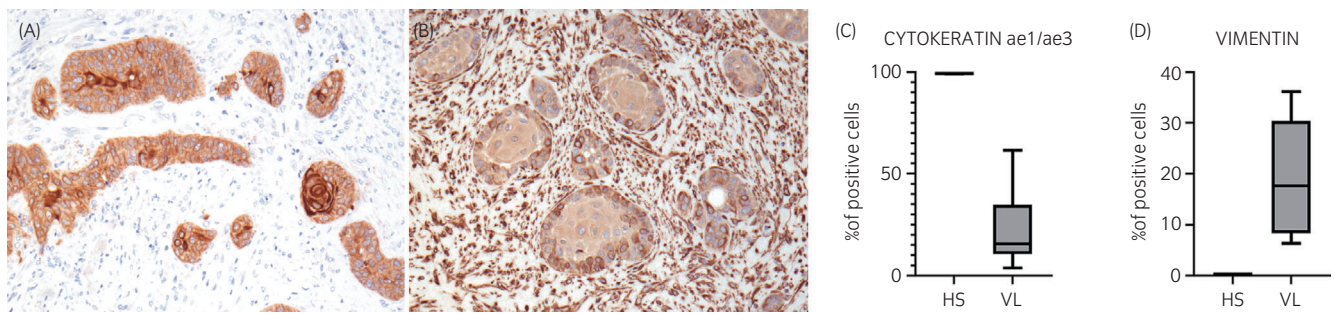


FIGURE 3 Immunohistochemistry (IHC) for cytokeratin AE1/AE2 (A) reveals a decreased expression within the neoplastic cells of VL (arrow). IHC for vimentin (B) often shows a cytoplasmic expression in VL sample (arrow). Box plots show a lower number of cells immunolabelled for cytokeratin AE1/AE2 in VL sample compared with HS (C). Box plots show a higher number of cells expressing vimentin within VL sample compared with HS sample (D). Scale bar = 100 μ m. HS, healthy skin; VL, vulvar lesion.

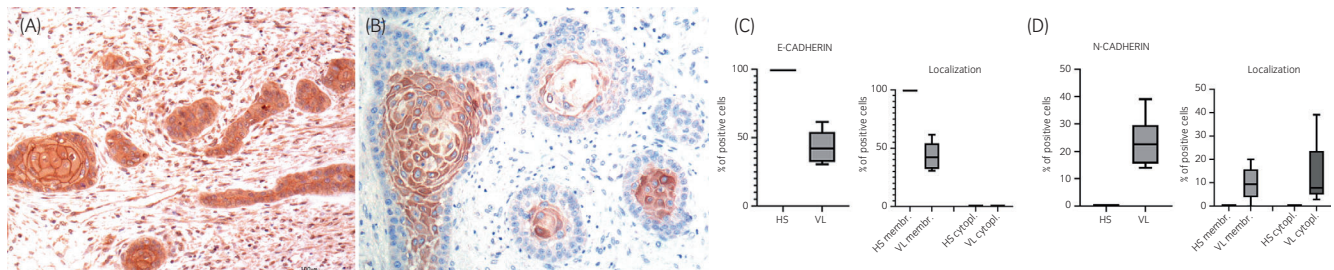


FIGURE 4 Immunohistochemistry (IHC) for E-cadherin (A) reveals a loss of E-cadherin expression at a membranous level within VL sample (arrow). IHC for N-cadherin reveals a higher number of cells expressing membranous (arrow) and cytoplasmic (arrowhead) N-cadherin in VL sample (B). Box plots show a lower number of cells immunolabelled for E-cadherin in VL compared with HS (C). Box plots showing HS sample with a higher number of cells expressing membranous E-cadherin with respect to VL sample (C). Box plots show a higher number of cells immunolabelled for N-cadherin in VL sample compared with HS sample (D). Box plots showing a higher number of cells expressing membranous and cytoplasmic N-cadherin in VL (D). Scale bar = 100 μ m. HS, healthy skin; VL, vulvar lesion.

with HS (Figure 5A,C). Finally, VL showed a significant ($p < 0.001$) higher number of cells expressing HIF1 α at a nuclear level with respect to HS (Figure 5B,D). A slightly higher percentage of Ki67-positive cells was found in VL when compared with HS (Figure 6A,B).

4 | DISCUSSION

Based on the current findings, a vulvar squamous cell carcinoma (VSCC) associated with EcPV2 infection was diagnosed. VSCC is a rare phenomenon in horses^{3,4,21,22} and has not been previously described in detail in Italy. In this case, in agreement with previous studies,^{3,4,22} we demonstrated the presence of EcPV2 RNA together with the expression of *L1*, *E6* and *E7* genes within the vulvar neoplastic lesion demonstrated also by RNAScope. Although both VL and HS were positive for EcPV2-*L1*, -*E6* and -*E7* DNA, only VL samples showed the gene expression of *L1*, *E6* and *E7*. The presence of viral DNA without viral gene expression within HS could be indicative of contamination by EcPV2 rather than a viral infection. Concerning the EcPV2-*E2* gene, all VL samples tested negative, not only for gene expression but also for DNA. This gene plays a pivotal role in virus replication and *E6/E7* regulation. In this respect, it is known that

during the early phase of infection, viral genome can be integrated into the host DNA or maintained as multiple episomes that replicate together with the cells. However, the expression of viral *E1* and *E2* genes is required for initiating viral replication. Indeed, *E2* binding is essential for the recruitment of *E1* helicase, which in turn binds to cellular proteins necessary for DNA replication.²³ The lack of the *E2* gene in our case could be most likely due to virus genome integration within the host genome. It is known that *E2* can regulate and control the expression of the viral oncogenes (*E6* and *E7*) acting as a transcription factor in humans, thus this is a relevant finding also for the equine species. The total or partial loss of this gene, due to the integration, can determine the lack of transcriptional regulation of these oncogenes, increased transcription of which is required for promoting HPV-induced carcinogenesis,²³ and in turn is a consistent feature in invasive vulvar carcinoma.²³ Moreover, *E6* and *E7* are reported to be involved in the immune response modulation and in the EMT phenomenon.^{24–27} EMT represents a complex process through which, following the activation of key transcription factors (TWIST, ZEB, SNAIL1 and SLUG), epithelial cells transiently lose their differentiated features and acquire a mesenchymal phenotype.¹⁰ Thus far, EMT has been investigated in equine penile¹⁴ and laryngeal SCC,²⁰ but currently there are no available data for EMT in equine VSCC.

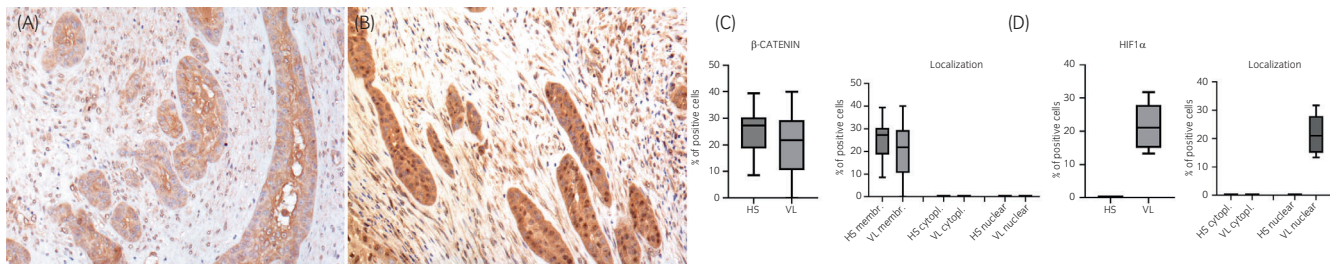


FIGURE 5 Immunohistochemistry (IHC) for β -catenin reveals a loss of expression at a membranous level within the neoplastic cells of VL (arrow) (A). IHC for HIF1 α reveals expression at a nuclear level within VL sample (B). Box plots show a slightly lower number of cells expressing β -catenin in VL (C). Box plots showing HS sample with a higher number of cells expressing membranous β -catenin (C). Box plots show a higher number of cells immunolabelled for HIF1 α (D). Box plots showing HS sample higher number of cells expressing HIF1 α at a nuclear level (D). Scale bar = 100 μ m. HS, healthy skin; VL, vulvar lesion.

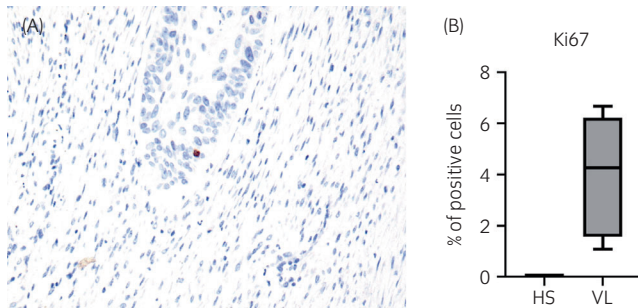


FIGURE 6 Immunohistochemistry for Ki67 showing nuclear positivity in the neoplastic cells of VL sample (A). Box plots showing a higher number of cells expressing Ki67 in VL sample compared with HS sample (B). Scale bar = 100 μ m. HS, healthy skin; VL, vulvar lesion.

Immunohistochemical analysis revealed a decreased expression of epithelial markers within the VL, together with an increased number of cells positive for mesenchymal markers. Interestingly, there was a significantly lower number of cells expressing cytokeratin within the neoplastic tissue, while scattered neoplastic cells with mesenchymal phenotype showed a cytoplasmic vimentin expression. Noteworthy, the number of cells expressing N-cadherin both at a cytoplasmic and membranous level was found to be increased, while cells expressing membranous E-cadherin were significantly decreased within the tumour. This finding might be suggestive of so-called “cadherin switching”, one of the distinctive features of EMT. Through this process, the E-cadherin adhesion molecule is replaced by N-cadherin, which endows neoplastic cells with migratory and invasive ability.^{7,11}

N-cadherin is a molecule naturally expressed by numerous cell types, including neural cells, endothelial cells, stromal cells and osteoblasts.²⁸ While N-cadherin is typically absent or poorly expressed in normal epithelial cells, its increased and aberrant expression within neoplastic cells has been associated with the development of various types of carcinoma^{28,29} and correlated with tumour aggressiveness.²⁸ Consistent with immunohistochemical analysis, gene expression results revealed an upregulation of *CDH2* and a down-regulation of *CDH1*, thus confirming the presence of an EMT phenotype at the mRNA level. All these findings were further supported by numerous

neoplastic cells displaying nuclear staining for hypoxia inducible factor 1 α (HIF-1 α). Most recently, the term hypoxia-induced EMT has been proposed, since the two events, hypoxia and EMT seem inter-related.³⁰ Indeed, HIF-1 α has been proved to modulate several EMT- transcription factors, including TWIST, Snail, Slug, SIP1 and ZEB1.³⁰ Interestingly, HIF-1 α could initiate EMT both directly, by binding to the proximal promoter of ZEB1 or TWIST via hypoxia response element,^{31,32} and indirectly, through the FoxM1 signalling pathway in prostate cancer cell lines³³ or through the *PAFAH1B2* gene in pancreatic cancer.³⁴

Results obtained by IHC were suggestive of EMT occurring within the neoplastic tissue. However, further investigations should be carried out to provide further insights into this complex and dynamic process and its underlying pathways.

Concerning the immune response, we observed a dense inflammatory reaction mostly consisting of neutrophils, and so we decided to investigate the gene expression of *CXCL8* and *IL12* family cytokines. We showed a significant increase of *CXCL8* gene expression (about 290 times) in VL compared with HS.

IL-8 is involved in cancer progression and metastases via various mechanisms, including pro-angiogenesis and the maintenance of cancer stem cells. IL-8 attracts and functionally modulates macrophages and neutrophils in tumour lesion, and triggers the extrusion of neutrophil extracellular traps.³⁵ A recent study in humans demonstrated high levels of IL-8 secretion by neutrophils with N2, pro-tumorigenic, phenotype.³⁶ The polarisation of tumour neutrophils in anti-tumorigenic N1 and pro-tumorigenic N2 phenotype was first proposed by Shaul and Fridlender.³⁷ N1 and N2 populations are defined based on their functional phenotype because to date no specific cell surface markers have been identified.

Recent evidence suggested the involvement of IL-27 in N phenotype³⁵: IL-27 is one of the IL-12 family cytokines, which, together with IL-12, IL-23 and IL-35, was investigated in this study for gene expression. All these ILs are produced by macrophages and dendritic cells³⁸ and, in our case, we can speculate that *IL27* is upregulated and *IL12* downregulated. As expected *IL27* was associated with the down-regulation of *IL17*; indeed, many studies have identified various immunosuppressive effects of IL-27 signalling, including suppression of TH17 differentiation.³⁹

In conclusion, with this case, we describe for the first time the EMT process in equine vulvar SCC associated with EcpV2 infection.

Our data demonstrated high levels of gene expression for CXCL8 and suggested a possible modulation of the IL-12 superfamily associated with the down-regulation of Th17.

AUTHOR CONTRIBUTIONS

All authors contributed to study design, study execution, data analysis and interpretation, preparation of the manuscript and final approval of the manuscript. All authors had full access to all the data in the study and take responsibility for the integrity of the data and the accuracy of the data analysis.

ACKNOWLEDGEMENTS

The authors thank Melania Di Pentima for her technical support. Open Access funding enabled and organized by Projekt DEAL.

FUNDING INFORMATION

This research was funded by the Italian Ministry of Health (Grant number IZS PLV 15/18 RC) and the Region of Liguria (Grant number 22L03); the article processing charge (APC) was funded by IZS PLV 15/18 RC and the Region of Liguria 22L03. This Open Access publication was funded by the Deutsche Forschungsgemeinschaft (DFG, German Research Foundation)—491094227 ‘Open Access Publication Funding’ and the University of Veterinary Medicine Hannover Foundation.

CONFLICT OF INTEREST STATEMENT

The authors declare no conflicts of interest.

PEER REVIEW

The peer review history for this article is available at <https://www.webofscience.com/api/gateway/wos/peer-review/10.1111/evj.13965>.

DATA AVAILABILITY STATEMENT

The data that support the findings of this study are available from the corresponding author upon reasonable request: Open sharing exemption granted by editor for this descriptive retrospective case report.

ETHICAL ANIMAL RESEARCH

Research ethics committee oversight not required by this journal: retrospective study of clinical records.

ETHICS STATEMENT

The study was conducted according to the guidelines of the Declaration of Helsinki and approved by the Institutional Ethics Committee of Istituto Zooprofilattico Sperimentale del Piemonte Liguria e Valle d'Aosta (Protocol Code 14047 of 11/28/2019).

INFORMED CONSENT

Owner gave explicit consent for inclusion of their animal in the report.

ORCID

Livia De Paolis  <https://orcid.org/0000-0002-8876-1853>

Chiara Guarnieri  <https://orcid.org/0000-0002-7033-0596>

Giuseppe Marruchella  <https://orcid.org/0000-0003-3176-3847>

REFERENCES

1. Van Den Top JGB, Ensink JM, Gröne A, Klein WR, Barneveld A, van Weeren PR. Penile and preputial tumours in the horse: literature review and proposal of a standardised approach. *Equine Vet J.* 2010; 42(8):746–57. <https://doi.org/10.1111/j.2042-3306.2010.00290.x>
2. Gupta S, Kumar P, Das BC. HPV: molecular pathways and targets. *Curr Probl Cancer.* 2018;42(2):161–74. <https://doi.org/10.1016/j.currprobcancer.2018.03.003>
3. Sykora S, Brandt S. Papillomavirus infection and squamous cell carcinoma in horses. *Vet J.* 2017;223:48–54. <https://doi.org/10.1016/j.tvjl.2017.05.007>
4. Porcellato I, Modesto P, Cappelli K, Varello K, Peletto S, Brachelente C, et al. Equus caballus papillomavirus type 2 (EcPV2) in co-occurring vulvar and gastric lesions of a pony. *Res Vet Sci.* 2020; 132:167–71. <https://doi.org/10.1016/j.rvsc.2020.06.003>
5. Scase T, Brandt S, Kainzbauer C, Sykora S, Bijmolt S, Hughes K, et al. Equus caballus papillomavirus-2 (EcPV-2): an infectious cause for equine genital cancer? *Equine Vet J.* 2010;42(8):738–45. <https://doi.org/10.1111/j.2042-3306.2010.00311.x>
6. Stratičò P, Razzuoli E, Hattab J, Guerri G, Celani G, Palozzo A, et al. Equine Gastric Squamous Cell Carcinoma in a Friesian Stallion. *J Equine Vet Sci.* 2022;117:104087. <https://doi.org/10.1016/j.jevs.2022.104087>
7. Lamouille S, Xu J, Derynck R. Molecular mechanisms of epithelial-mesenchymal transition. *Nat Rev Mol Cell Biol.* 2014;15(3):178–96. <https://doi.org/10.1038/nrm3758>
8. Micalizzi DS, Farabaugh SM, Ford HL. Epithelial-mesenchymal transition in cancer: parallels between normal development and tumor progression. *J Mammary Gland Biol Neoplasia.* 2010;15(2):117–34. <https://doi.org/10.1007/s10911-010-9178-9>
9. Cervantes-Arias A, Pang LY, Argyle DJ. Epithelial-mesenchymal transition as a fundamental mechanism underlying the cancer phenotype. *Vet Comp Oncol.* 2013;11(3):169–84. <https://doi.org/10.1111/j.1476-5829.2011.00313.x>
10. Chang H, Liu Y, Xue M, Liu H, Du S, Zhang L, et al. Synergistic action of master transcription factors controls epithelial-to-mesenchymal transition. *Nucleic Acids Res.* 2016;44(6):2514–27. <https://doi.org/10.1093/nar/gkw126>
11. Savagner P. The epithelial-mesenchymal transition (EMT) phenomenon. *Ann Oncol.* 2010;21(S7):vii89–92. <https://doi.org/10.1093/annonc/mdq292>
12. Armando F, Mazzola F, Ferrari L, Corradi A. An overview of epithelial-to-mesenchymal transition and mesenchymal-to-epithelial transition in canine tumors: how far have we come? *Vet Sci.* 2022;10(1):19. <https://doi.org/10.3390/vetsci10010019>
13. Al Moustafa AE. E5 and E6/E7 of high-risk HPVs cooperate to enhance cancer progression through EMT initiation. *Cell Adh Migr.* 2015;9(5):392–3. <https://doi.org/10.1080/19336918.2015.1042197>
14. Armando F, Mecocci S, Orlandi V, Porcellato I, Cappelli K, Mechelli L, et al. Investigation of the epithelial to mesenchymal transition (EMT) process in equine papillomavirus-2 (EcPV-2)-positive penile squamous cell carcinomas. *Int J Mol Sci.* 2021;22(19):10588. <https://doi.org/10.3390/ijms221910588>
15. Mecocci S, Porcellato I, Armando F, Mechelli L, Brachelente C, Pepe M, et al. Equine genital squamous cell carcinoma associated with EcPV2 infection: RANKL pathway correlated to inflammation and Wnt signaling activation. *Biology.* 2021;10(3):244. <https://doi.org/10.3390/biology10030244>
16. Strohmayr C, Klang A, Kummer S, Walter I, Jindra C, Weissenbacher-Lang C, et al. Tumor cell plasticity in equine papillomavirus-positive versus-negative squamous cell carcinoma of the head and neck. *Pathogens.* 2022;11(2):266. <https://doi.org/10.3390/pathogens11020266>
17. Suárez-Bonnet A, Willis C, Pittaway R, Smith K, Mair T, Priestnall SL. Molecular carcinogenesis in equine penile cancer: a potential animal model for human penile cancer. *Urol Oncol.* 2018;36(12):532.e9–532.e18. <https://doi.org/10.1016/j.urolonc.2018.09.004>

18. Cappelli K, Ciucis CGD, Mecocci S, Nervo T, Ines Crescio M, Pepe M, et al. Detection of equus caballus papillomavirus type-2 in asymptomatic Italian horses. *Viruses*. 2022;14(8):1696. <https://doi.org/10.3390/v14081696>
19. Porcellato I, Mecocci S, Mechelli L, Capelli K, Brachelente C, Pepe M, et al. Equine penile squamous cell carcinomas as a model for human disease: a preliminary investigation on tumor immune microenvironment. *Cell*. 2020;9(11):2364. <https://doi.org/10.3390/cells9112364>
20. Armando F, Godizzi F, Razzuoli E, Leonardi F, Angelone M, Corradi A, et al. Epithelial to mesenchymal transition (EMT) in a laryngeal squamous cell carcinoma of a horse: future perspectives. *Animals*. 2020;10(12):2318. <https://doi.org/10.3390/ani10122318>
21. Munday JS, Knight CG, Luff JA. Papillomaviral skin diseases of humans, dogs, cats and horses: a comparative review. Part 2: pre-neoplastic and neoplastic diseases. *Vet J*. 2022;288:105898. <https://doi.org/10.1016/j.tvjl.2022.105898>
22. Yamashita-Kawanishi N, Ito S, Chambers JK, Uchida K, Sato M, Chang HW, et al. Vulvar squamous cell carcinoma associated with Equus caballus papillomavirus type 2 infection in a Japanese mare. *Tumour Virus Res*. 2021;12:200226. <https://doi.org/10.1016/j.tvr.2021.200226>
23. Araldi RP, Sant'Ana TA, Módolo DG, de Melo GC, Spadacci-Morena DD, de Cassia Stocco R, et al. The human papillomavirus (HPV)-related cancer biology: an overview. *Biomed Pharmacother*. 2018;106:1537–56. <https://doi.org/10.1016/j.biopha.2018.06.149>
24. Barillari G, Bei R, Manzari V, Modesti A. Infection by high-risk human papillomaviruses, epithelial-to-mesenchymal transition and squamous pre-malignant or malignant lesions of the uterine cervix: a series of chained events? *Int J Mol Sci*. 2021;22(24):13543. <https://doi.org/10.3390/ijms222413543>
25. Chen X, Bode AM, Dong Z, Cao Y. The epithelial-mesenchymal transition (EMT) is regulated by oncoviruses in cancer. *FASEB J*. 2016;30(9):3001–10. <https://doi.org/10.1096/fj.201600388R>
26. Rezaei M, Mostafaei S, Aghaei A, Hosseini N, Darabi H, Nouri M, et al. The association between HPV gene expression, inflammatory agents and cellular genes involved in EMT in lung cancer tissue. *BMC Cancer*. 2020;20(1):916. <https://doi.org/10.1186/s12885-020-07428-6>
27. Zhou C, Tuong ZK, Frazer IH. Papillomavirus immune evasion strategies target the infected cell and the local immune system. *Front Oncol*. 2019;9:682. <https://doi.org/10.3389/fonc.2019.00682>
28. Mrozik KM, Blaschuk OW, Cheong CM, Zannettino ACW, Vandyke K. N-cadherin in cancer metastasis, its emerging role in haematological malignancies and potential as a therapeutic target in cancer. *BMC Cancer*. 2018;18(1):939. <https://doi.org/10.1186/s12885-018-4845-0>
29. Hui L, Zhang S, Dong X, Tian D, Cui Z, Qiu X. Prognostic significance of twist and N-cadherin expression in NSCLC. *PLoS One*. 2013;8(4):e62171. <https://doi.org/10.1371/journal.pone.0062171>
30. Tam SY, Wu WVC, Law HKW. Hypoxia-induced epithelial-mesenchymal transition in cancers: HIF-1 α and beyond. *Front Oncol*. 2020;10:486. <https://doi.org/10.3389/fonc.2020.00486> Accessed 13 Feb 2023.
31. Zhang W, Shi X, Peng Y, Wu M, Zhang P, Xie R, et al. HIF-1 α promotes epithelial-mesenchymal transition and metastasis through direct regulation of ZEB1 in colorectal cancer. *PLoS One*. 2015;10(6):e0129603. <https://doi.org/10.1371/journal.pone.0129603>
32. Yang MH, Wu MZ, Chiou SH, Chen P-M, Chang S-Y, Liu C-J, et al. Direct regulation of TWIST by HIF-1 α promotes metastasis. *Nat Cell Biol*. 2008;10(3):295–305. <https://doi.org/10.1038/ncb1691>
33. Tang C, Liu T, Wang K, Wang X, Xu S, He D, et al. Transcriptional regulation of FoxM1 by HIF-1 α mediates hypoxia-induced EMT in prostate cancer. *Oncol Rep*. 2019;42(4):1307–18. <https://doi.org/10.3892/or.2019.7248>
34. Ma C, Guo Y, Zhang Y, Duo A, Jia Y, Liu C, et al. PAFAH1B2 is a HIF1 α target gene and promotes metastasis in pancreatic cancer. *Biochem Biophys Res Commun*. 2018;501(3):654–60. <https://doi.org/10.1016/j.bbrc.2018.05.039>
35. Xiong S, Dong L, Cheng L. Neutrophils in cancer carcinogenesis and metastasis. *J Hematol Oncol*. 2021;14(1):173. <https://doi.org/10.1186/s13045-021-01187-y>
36. Ohms M, Möller S, Laskay T. An attempt to polarize human neutrophils toward N1 and N2 phenotypes in vitro. *Front Immunol*. 2020;11:532. <https://doi.org/10.3389/fimmu.2020.00532>
37. Shaul ME, Fridlender ZG. Tumour-associated neutrophils in patients with cancer. *Nat Rev Clin Oncol*. 2019;16(10):601–20. <https://doi.org/10.1038/s41571-019-0222-4>
38. Habiba U e, Rafiq M, Khawar MB, Nazir B, Haider G, Nazir N. The multifaceted role of IL-12 in cancer. *Adv Cancer Biol Metastasis*. 2022;5:100053. <https://doi.org/10.1016/j.adcanc.2022.100053>
39. Morita Y, Masters EA, Schwarz EM, Muthukrishnan G. Interleukin-27 and its diverse effects on bacterial infections. *Front Immunol*. 2021;12:678515. <https://doi.org/10.3389/fimmu.2021.678515>

SUPPORTING INFORMATION

Additional supporting information can be found online in the Supporting Information section at the end of this article.

How to cite this article: De Paolis L, Armando F, Montemurro V, Petrizzi L, Straticò P, Mecocci S, et al. Epithelial-mesenchymal transition in an EcPV2-positive vulvar squamous cell carcinoma of a mare. *Equine Vet J*. 2023. <https://doi.org/10.1111/evj.13965>